# Numerical analysis of heat transfer in the exhaust gas flow in a diesel power generator

# Numerical analysis of heat transfer in the exhaust gas flow in a diesel power generator

**C H G Brito[1], C B Maia[2] and J R Sodré[3]**

Postgraduate Program in Mechanical Engineering, Pontifical Catholic University of Minas Gerais, Av. Dom José Gaspar, 500, Belo Horizonte, MG, 30535-901, BR

Email: cristianohbrito@globo.com[1]; cristiana@pucminas.br[2]; ricardo@pucminas.br[3]

**Abstract**. This work presents a numerical study of heat transfer in the exhaust duct of a diesel power generator. The analysis was performed using two different approaches: the Finite Difference Method (FDM) and the Finite Volume Method (FVM), this last one by means of a commercial computer software, ANSYS CFX®. In FDM, the energy conservation equation was solved taking into account the estimated velocity profile for fully developed turbulent flow inside a tube and literature correlations for heat transfer. In FVM, the mass conservation, momentum, energy and transport equations were solved for turbulent quantities by the K-ω SST model. In both methods, variable properties were considered for the exhaust gas composed by six species: $CO_2$, $H_2O$, $H_2$, $O_2$, CO and $N_2$. The entry conditions for the numerical simulations were given by experimental data available. The results were evaluated for the engine operating under loads of 0, 10, 20, and 37.5 kW. Test mesh and convergence were performed to determine the numerical error and uncertainty of the simulations. The results showed a trend of increasing temperature gradient with load increase. The general behaviour of the velocity and temperature profiles obtained by the numerical models were similar, with some divergence arising due to the assumptions made for the resolution of the models.

## 1. Introduction

The study of heat transfer in internal combustion engines is an important requirement to improve engine performance and control pollutant emissions [1]. Many researches give a special focus to the exhaust system to assess energy availability, heat transfer from the exhaust gas and optimal points of device installation [2,3]. The gas flow dynamics in the exhaust pipe has been studied to verify the influence of heat transfer on catalyst efficiency, confirming that the control of temperature for cold start is fundamental to catalyst performance [3]. A computational fluid dynamics (CFD) simulation verified that the monolithic reactors used in catalysts for exhaust gas post-treatment are strongly influenced by fluctuations in the conditions of the flow generated by the engine pulse and turbulence [4]. Studies using CFD simulation showed that heat transfer in the exhaust system is directly related to engine emissions [5]. CFD simulation allows the formulation of the heat transfer problem in engine exhaust systems [6], the prediction of heat transfer mechanisms in different engine configurations, and the evaluation of exergy destruction rate in the exhaust gas [7].

The analysis of the governing equations of fluid flow and temperature profiles results in complex calculations and difficult analytical solution. The application of numerical methods, such as the finite difference method (FDM) and the finite volume method (FVM), can be solve the problem. The FDM is a numerical method largely used to study heat transfer and fluid flow dynamics [8]. The FDM was employed to verify the energy availability of the exhaust gas [9] and evaluate the influence of heat

transfer on engine performance [2,9]. FDM modelling of the exhaust gas flow showed that thermal conduction is the major heat transfer mechanism in the particle filter of the exhaust system [10]. Heat transfer modelling was performed via FDM to obtain the temperature profiles of the exhaust gas [11]. The exhaust gas fluid flow and heat transfer were simulated via FDM to optimize the exhaust system design [12].

Thus, the objective of this work is to develop a FDM based model to evaluate heat transfer in the exhaust pipe of an engine and compare the results with FVM modelling using a commercial software, Ansys CFX. The FDM model considers turbulent fluid flow and variable flow properties for resolution of the energy equation and determination of temperatures profiles of the exhaust gas. In both numerical models, the exhaust gas was considered to be composed by six species: carbon dioxide ($CO_2$), water vapour ($H_2O$), hydrogen ($H_2$), oxygen ($O_2$), carbon monoxide (CO) and nitrogen ($N_2$). The numerical simulation was carried out for engine operation under loads from 0 kW to 37.5 kW, according to ASME V & V 20-2009 standard.

## 2. Problem formulation

The exhaust system is responsible by about 30% of energy loss from internal combustion engines [12]. The energy carried by the exhaust gas can be evaluated from analysis of the internal fluid flow. The determination of heat loss through the exhaust system is important for engine efficiency improvement though the application of heat recovery devices and optimization of emission control devices. Figure 1 shows the physical domain. The heat transfer and fluid flow is analysed approaching the duct to a straight pipe in FDM model (Fig. 2) and considering the existence of the curve in the FDV model (Fig. 3). The reference points and dimensions indicated in Fig. 3 are used in both models.

**Figure 1.** Exhaust pipe

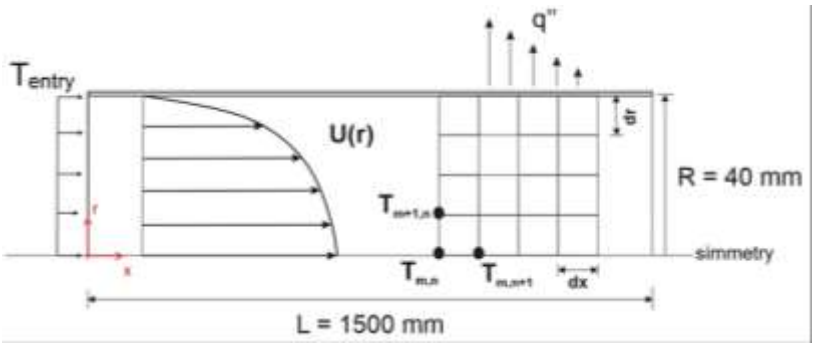


**Figure 2.** Computational domain of FDM model

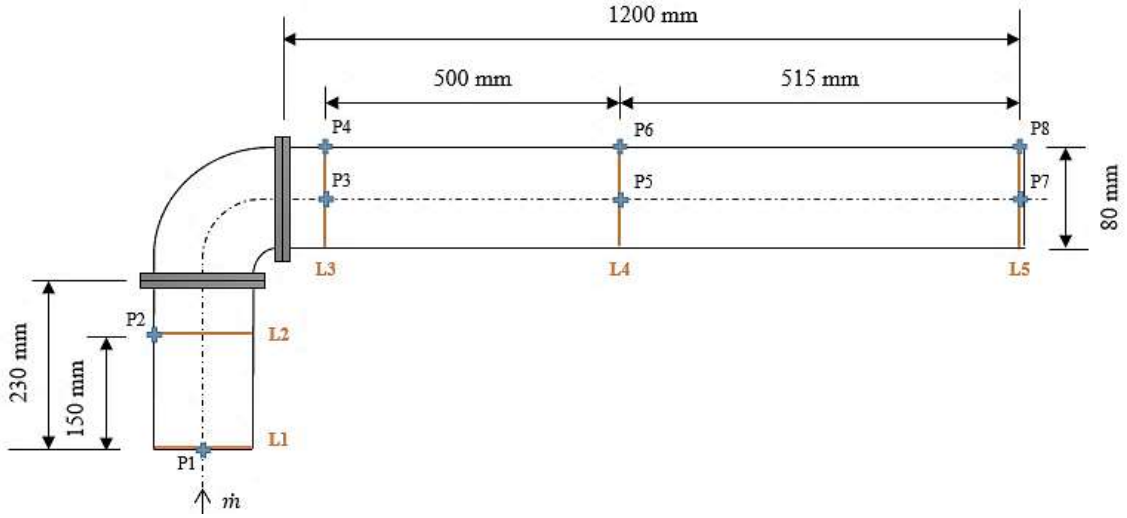


**Figure 3.** Computational domain of CFD model

## 3. Mathematical model

To determine the temperature profiles a FDM based model was developed. The implemented FDM model solve the energy equation from the fundamental assumptions: steady state, fully developed turbulent flow; one-seventh power profile for the velocity; variable properties; fluid modelled as exhaust gas with six species; ideal gas. The results of this model are compared with results obtained from the FVM based Ansys CFX® software, in which the governing equations of turbulent flow were resolved from the fundamental assumptions: steady state, turbulent flow; K-ω SST turbulence model; fluid modelled as exhaust gas with six species; ideal gas.

### 3.1. Governing equations

The governing equations of turbulent fluid flow are [13]:

- Continuity equation

$$\frac{\partial}{\partial t}\rho + \nabla \bullet \left(\rho \overline{\mathbf{U}}\right) = 0 \tag{1}$$

- Momentum equation

$$\frac{D\left(\rho \overline{\mathbf{U}}\right)}{Dt} = \rho \mathbf{g} - \nabla \overline{p} + \nabla \bullet \tau_{ij} \tag{2}$$

- Energy equation

$$\rho c_p \frac{D\overline{T}}{Dt} = -\frac{\partial}{\partial x_i} q_i + \overline{\Phi} \tag{3}$$

- Ideal gas state equation

$$\overline{p} = \rho R \overline{T} \tag{4}$$

Where, $\rho$ is fluid density, $\overline{\mathbf{U}}$ is velocity, $\mathbf{g}$ is gravity acceleration, $\overline{p}$ is pressure, $\tau_{ij}$ is Reynolds stress tensor, $c_p$ is specific heat, $\overline{T}$ is temperature, $q_i$ is heat flux, $\overline{\Phi}$ dissipation viscous function, $t$ is time coordinate and $R$ is ideal gas constant.

The K-ω SST model is used to treat the turbulent regime in the present study.

## 4. Numerical methodology

In this research, two numerical methods were used to determine the temperature profiles of the exhaust gas. The FDM was used to solve the energy equation and the FVM was used to solve governing equations of turbulent flow. In both models, the exhaust gas was modelled with six species: (1) $CO_2$; (2) CO; (3) $O_2$; (4) N2; (5) $H_2O$ and (6) $H_2$, and constant composition along of the pipe.

### *4.1. FDM model*

To solve the energy equation (Eq. 3), in FDM model, the following hypotheses were adopted: (1) steady state; (2) two dimensional heat transfer axisymmetric; (3) turbulent fully developed flow; (4) one-seventh power profile for the velocity [16]; (5) variable properties; (6) fluid modelled with exhaust gas with six species. To discretize the energy equation, based on FDM, the bi-dimensional nodal mesh exemplified in Fig. 2 was used. For the discretization of the energy equation, it is necessary to perform the analysis into two distinct regions: internal volumes and border volumes (close to the walls).

To analyse the region between the centreline and the pipe wall, the energy equation is written as

$$\rho(T) c_p(T) u \frac{\partial T}{\partial x} = \frac{1}{r} \cdot k(T) \cdot \frac{\partial T}{\partial r} + k(T) \cdot \frac{\partial^2 T}{\partial r^2} \qquad \rightarrow \qquad 0 < r < R \tag{5}$$

Where $k$ is the thermal conductivity.

The Eq. (14) is a nonlinear convection-diffusion equation. Due to the presence of the convection term, it uses the upwind method to avoid numerical instability and diffusion [17]. The discretized form is

$$F(T)\cdot u_{m,n}\frac{T_{m,n-1}-T_{m,n}}{\Delta x}=\frac{G_1(T)}{m}\cdot\frac{T_{m+1}-T_{m,n}}{\Delta r}+G_2(T)\cdot\frac{T_{m+1,n}-2\cdot T_{m,n}+T_{m-1,n}}{(\Delta r)^2} \quad \textbf{(6)}$$

Where $u_{m,n}$ calculates from one-seventh power profile for the velocity [16], $m$ indicates radial position and $n$ indicates axial position of the node, and $F(T)$, $G_1(T)$ and $G_2(T)$ are functions to simplify the equations, written as

$$F(T)=\frac{\rho(T_{m,n+1})\cdot c_p(T_{m,n+1})+\rho(T_{m,n})\cdot c_p(T_{m,n})}{2}$$

$$G_1(T)=\frac{k(T_{m+1,n})+k(T_{m,n})}{2} \qquad G_2(T)=\frac{k(T_{m+1,n})+k(T_{m,n})+k(T_{m-1,n})}{3} \quad \textbf{(7)}$$

In the centreline, the energy equation can be written as [17]

$$\rho(T)\,c_p(T)\,u\frac{\partial T}{\partial x}=2\cdot k(T)\frac{\partial^2 T}{\partial r^2} \qquad \rightarrow \qquad r=0 \quad \textbf{(8)}$$

The discretized equation takes the following form

$$F(T)\cdot\frac{T_{m,n-1}-T_{m,n}}{\Delta x}=2\cdot G_2(T)\cdot\frac{T_{m+1,n}-2\cdot T_{m,n}+T_{m-1,n}}{(\Delta r)^2} \quad \textbf{(9)}$$

In the pipe surface the heat flux balance is null [17], thus

$$\int_s \mathbf{q}\cdot\mathbf{n}\,ds=0 \quad \textbf{(10)}$$

Heat transfer in the pipe wall is given by internal convection, due to the exhaust gas flow, and by natural convection due to contact with outside air. The heat flux balance results

$$T_{m,n}=\frac{h_f}{h_\infty+h_f}T_{m+1,n}+\frac{h_\infty}{h_\infty+h_f}T_\infty \quad \textbf{(11)}$$

On which the internal heat transfer coefficient, $h_f$, is given by Gnielinski correlation [15] and the natural heat transfer coefficient, $h_\infty$, is given by Churchill and Chu correlation [15].

*4.1.1. Algorithm*

The FDM, implemented in Matlab 2013 algorithm, was used to solve the energy equation. The flowchart shown in Figure 4 presents the iterative calculation process. As convergence criterion it was adopted [17]

$$\left|\frac{T^{k+1}-T^k}{T^k_{\max}-T^k_{\min}}\right|\le\varepsilon \quad \textbf{(12)}$$

To determine the equations of the intensive properties of the fluid as a function of temperature, the software EES® - Engineering Equation Solver was used for numerical regression with temperature values ranging from 100 K to 1200 K, comprising the temperature range observed in the exhaust duct.

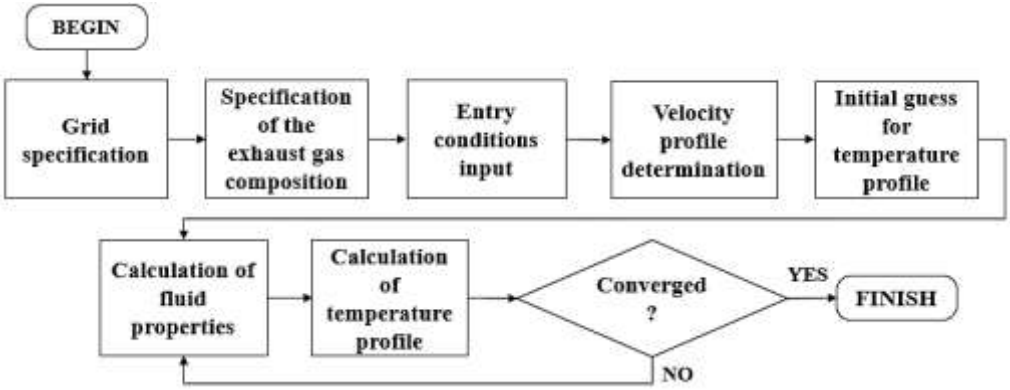


**Figure 4.** Algorithm flowchart

*4.2. FVM model*

The FVM model was solved with Ansys CFX® 14.5 software from the adoption of the pipe geometry exemplified in Fig. 3, 3-D fluid dynamics and heat transfer. This model was solved to be compared with the FDM model. The entry conditions were output with relative static pressure of 0 Pa; non-sliding wall condition; mass flow rate measured experimentally; gas temperature measured experimentally; prescribed heat transfer coefficient in the duct wall; ambient temperature 27°C.

4.3. Entry data of numerical models

In the numerical simulations, the adopted input and boundary conditions obtained experimentally are described in Table 1, with the diesel power generator operating under variable loads. The rotational speed of the engine was maintained constant at 1800 rpm.

**Table 1.** Entry data used in the numerical simulations

| Load | Temperature (°C) | | Mass fraction (%) | | | | | |
|---|---|---|---|---|---|---|---|---|
| (kW) | Ambient (°C) | Inlet (°C) | $CO_2$ | CO | $O_2$ | $N_2$ | $H_2O$ | $H_2$ |
| 0 | 33.4 | 178.0 | 5.1 | 0.0365 | 16.2 | 76.5 | 2.2 | 0.0000 |
| 10 | 34.4 | 264.5 | 6.6 | 0.0321 | 14.8 | 75.9 | 2.8 | 0.0000 |
| 20 | 34.9 | 369.0 | 9.9 | 0.0238 | 11.4 | 74.5 | 4.2 | 0.0000 |
| 37.5 | 31.9 | 579.2 | 16.2 | 0.0852 | 5.4 | 72.1 | 6.1 | 0.0896 |

## 5. Results and discussion

The algorithm implemented in Matlab had as input parameters the values reported in Table 1. For the velocity profile, it was proposed to use one-seventh power profile. The relative convergence criterion adopted has the value of 1%. Mesh tests were performed according to ASME V&V 20-2009 standard. Simulations were performed in five meshes, reducing the element size from a constant factor. The mesh with 0.430 mm element size was considered converged. The simulated FVM model in Ansys CFX® 14.5 also had as input parameters the values reported in Table 1. Mesh tests were performed at the point P8 indicated in Fig. 2. The mesh with 11.6 million elements was considered converged when the residual convergence was $10^{-6}$.

The axial temperature distribution in the exhaust pipe is presented in Fig. 5 with numerical uncertainties indicates by error bars. The temperature in the centreline (Tc) has different behaviour for each of the numerical models. In the FDM model, it was not observed temperature reduction, due to the hypothesis of turbulent, fully developed flow. In the FVM model, a reduction of Tc was observed. However, temperature reduction occurs rapidly between the axial positions 400 and 600 mm, in the elbow position. After the elbow, the temperature is increased probably due to gas recirculating in this region and heat transfer intensification. The wall temperature (Tp) shows a similar behaviour for both models, with reducing values along the axial length. However, the FDM model underestimates the heat flux along the duct, leading to lower temperature gradients. This behaviour may be explained by the fact

that turbulent thermal diffusion was not taken into account. In the FVM model, the wall temperature presents a similar behaviour as the centreline temperature. After the bend, the wall temperature undergoes a slight increase and, then, it decreases again.

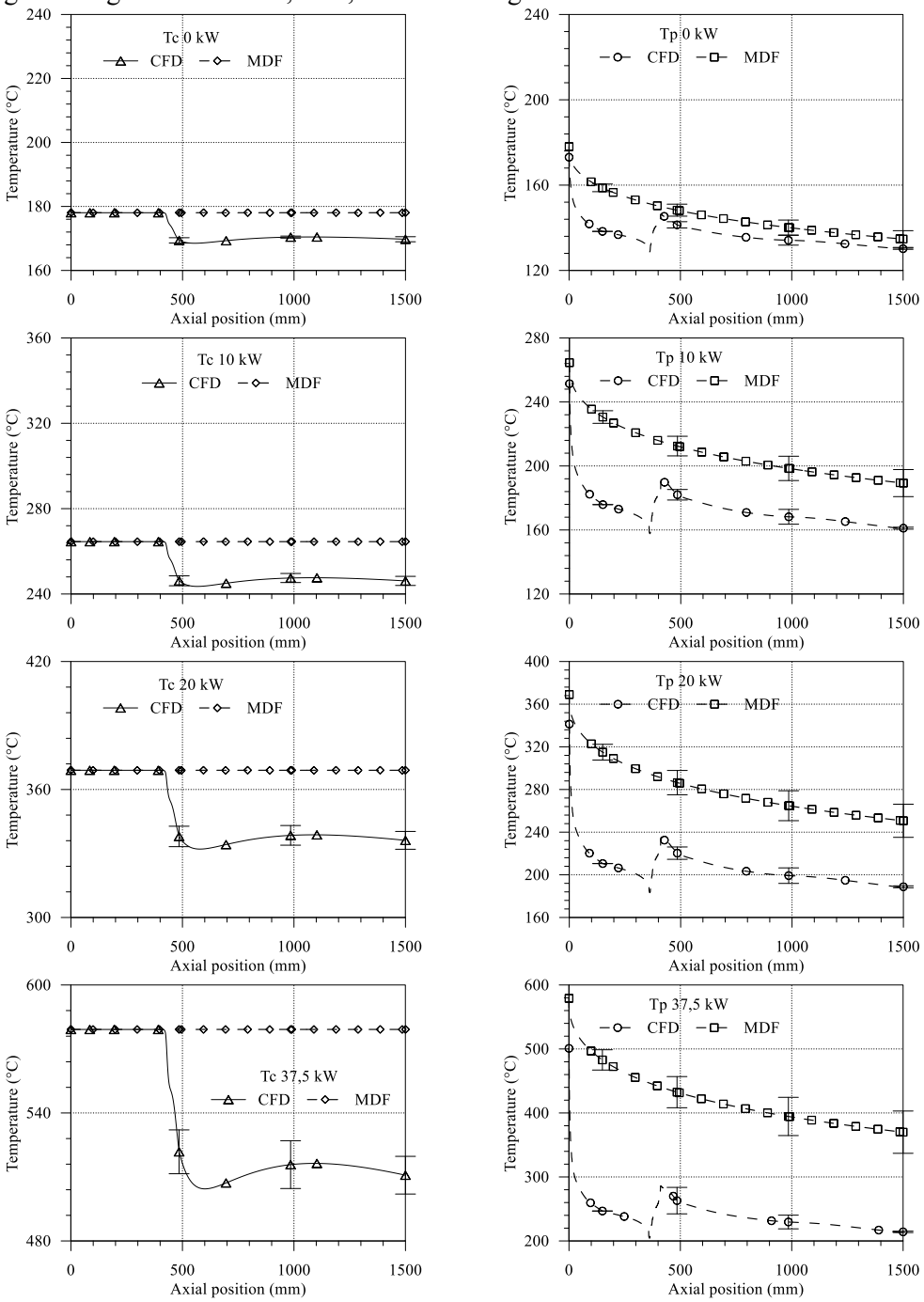


**Figure 5.** Axial temperature distribution

Figure 6 shows that the radial temperature profiles obtained from each model are not similar. The FDM produced a radially symmetric temperature profile throughout the duct while the FVM temperature profile undergoes a contraction due to change of flow direction and recirculation gas imposed by the elbow. The FDM model underestimates heat transfer along the duct when compared to the FVM model. In the region upstream the elbow, 0 mm and 150 mm, the models predict a very close temperature

profile. Downstream the elbow, 485 mm to 1500 mm, the temperature profile predicted by the FDM model deviates significantly from the profile predicted by the FVM model due to the inability of the FDM model to predict the heat transfer intensification resulted from the high turbulence in this region. It should be noted that the symbols shown does not correspond to nodal mesh that have a much larger number of points.

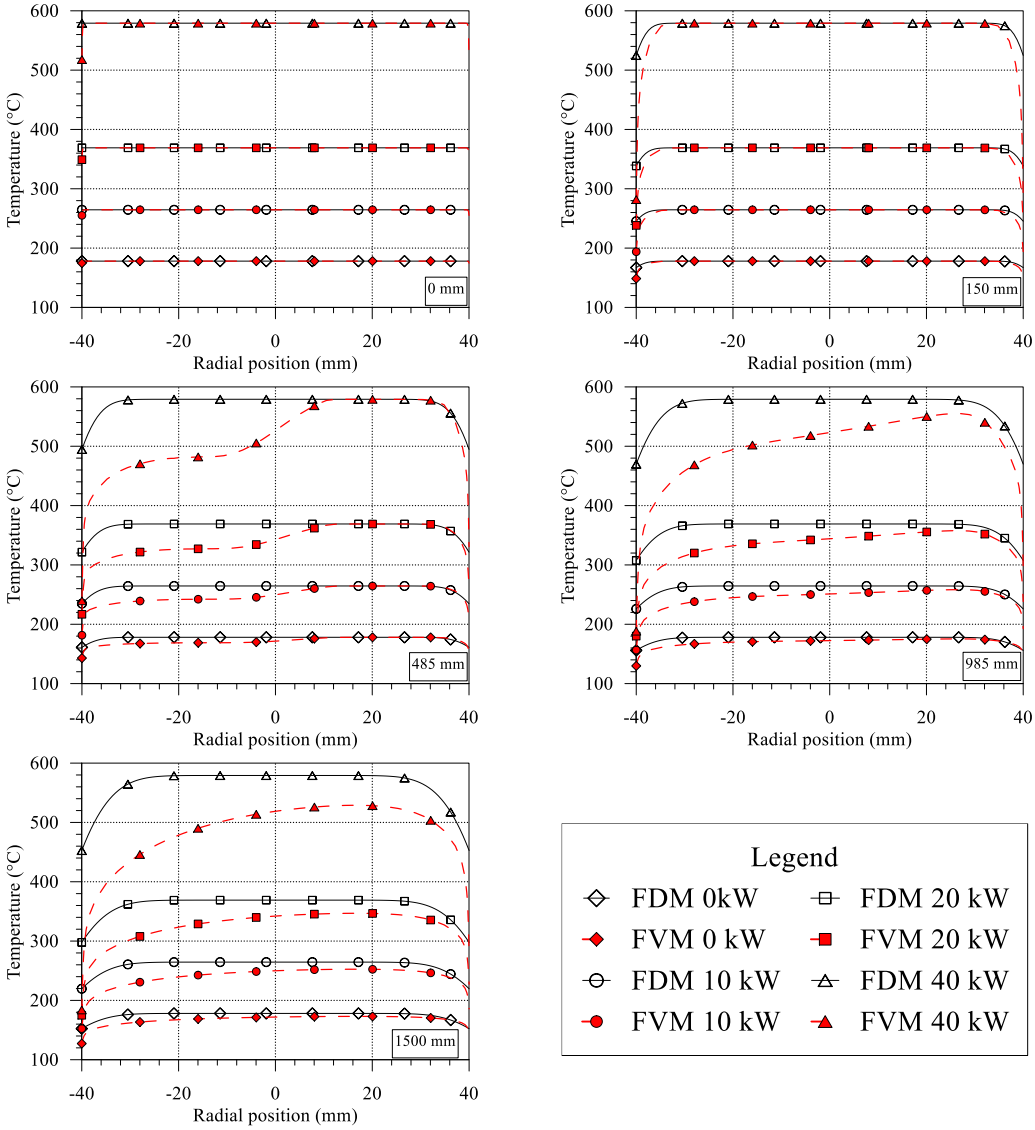


**Figure 6.** Radial temperature profiles

## 6. Conclusions

With the numerical methodology employed, it was possible to determine the temperature profiles in the exhaust duct of a diesel power generator operating at different workloads. The FDM and FVM models showed agreement in predicting increased temperature gradient with increased engine load, although the estimate of temperature distribution is significantly different for each model. Disagreement in predicting the behaviour of temperature profiles is first because the FDM model adopts a simplified duct geometry and, therefore, does not anticipate a change in flow direction. Second, the consideration of fully developed flow causes the FDM model to underestimate heat transfer along the exhaust duct. When compared with the FVM model, the flow is seen to be strongly turbulent in the region immediately after the curve, in addition to not being developed due to the presence of the curve, thus enhancing the heat flux.

It is concluded that the FVM model is more suitable for detailed analysis of the temperature distribution inside the exhaust duct. However, the FDM can be recommended for a preliminary analysis, given the complexity of the various stages of a FVM analysis. The elbow is a sensitive region of the exhaust duct, since it significantly affects fluid flow, generating high turbulence and intensifying heat transfer. The installation of devices in the exhaust system must consider it. Heat recovery devices need a large amount of energy and should be installed upstream the elbow. Recirculation devices that require low temperatures can be installed downstream the elbow.

## 7. Acknowledgments

The authors thank CAPES, CNPq research project 304114/2013-8, FAPEMIG research project TEC PPM 0385-15 and VALE/FAPEMIG research project TEC RDP 00198-10 for the financial support to this work.

## References

[1] Drenth A C, Olsen D B, Cabot P E and Johnson J J 2014 Compression ignition engine performance and emission evaluation of industrial oilseed feedstock camelina, carinata and pennycress across three fuel pathways *Fuel* **136** 143-155
[2] Galindo J, Luján J M, Serrano J R, Dolz V, Guilain S 2006 Description of a heat transfer model suitable to calculate transient processes of turbocharged diesel engines with one-dimensional gas dynamic codes *Energy* **43** 201-213
[3] Another reference Gasser I, Rybicki M 2013 Modelling and simulation of gas dynamics in an exhaust pipe *Applied Mathematical Modelling* **37** 2747-2764
[4] Ström H, Sasic S 2013 Heat and mass transfer in automotive catalysts – The influence of turbulence velocity fluctuations *Chemical Engineering Science* **83** 128-137
[5] Rakopoulos C, Kosmadakis G M, Demuynck J, Paepe M, Verhelst S 2011 A combined experimental and numerical study of thermal processes, performance and nitric oxide emissions in a hydrogen-fueled spark-ignition engine *International Journal of Hydrogen Energy* **36** 5163-5180
[6] Rakopoulos C, Kosmadakis G and Pariotis E 2010 Critical evaluation of current heat transfer models used in CFD in-cylinder engine simulations and establishment of a comprehensive wall-function formulation *Applied Energy* **87** 1612-1630
[7] Sekavcnik M, Ogoreve T, Katrasnik T and Rodman-Opresnik S 2012 Three-dimensional approach to exhaust gas energy analysis *Heat Mass Transfer* **48** 923-931
[8] Maliska C R 1995 *Computational Heat Transfer and Fluid Mechanics* (Rio de Janeiro: LTC)
[9] Rakopoulos C, Andritsakis E, Hountalas D 1995 The influence of exhaust system unsteady gas flow and insulation on the performance of turbocharged diesel *Heat Recovery Systems & CHP* **15** 51-72
[10] Galindo J, Serrano J R, Piqueras P, García-Afonso O 2012 Heat transfer modelling in honeycomb wall-flow diesel particulate filters *Energy* **43** 201-213
[11] Luján J M, Climent H, Olmeda P and Jimenéz V D 2014 Heat transfer modeling in exhaust system of high-performance two-stroke engines *Applied Thermal Engineering* **69** 96-104
[12] Kesgin U 2005 Study on the design of inlet and exhaust system of a stationary internal combustion engine *Energy Conversion and Management* **46** 2258-2287
[13] Pulkrabek W W 1997 *Engineering Fundamentals of the Internal Combustion Engine* (New Jersey: Pratice Hall) pp 312
[14] Versteeg H K and Malalasekera W (2007) *An Introduction to Computational Fluid Dynamics: The Finite Volume Method* 2. Ed. (London: Pearson Education)
[15] Bejan A (2012) *Convective Heat Transfer* 2. Ed. (New Jersey: John Wiley & Sons)
[16] White F (2007) *Fluid Mechanics* 6. Ed. (New York: McGraw-Hill)
[17] Özisik N (1994), *Finite Difference Methods in Heat Transfer,* (Florida : CRC Press)